Ketonic Defects in Ladder-type Poly(*p*-phenylene)s

Lorenz Romaner,[†,‡] Georg Heimel,[§] Herbert Wiesenhofer,[§] Patricia Scandiucci de Freitas,[||] Ullrich Scherf,[||] Jean-Luc Brédas,[*,†] Egbert Zojer,[*,†,§] and Emil J. W. List[*,‡]

School of Chemistry and Biochemistry, Georgia Institute of Technology, 770 State Street, Atlanta, Georgia 30332-0400, Institute of Solid State Physics, Graz University of Technology, Petersgasse 16, A-8010 Graz, Austria, Bergische Universität Wuppertal, Makromolekulare Chemie, Fachbereich Chemie, Gauss-Str. 20, D-42097 Wuppertal, Germany, and Christian Doppler Laboratory—Advanced Functional Materials, Institute of Nanostructured Materials and Photonics, Joanneum Research, A-8160 Weiz, and Institute of Solid State Physics, Graz, University of Technology, Petersgasse 16/I/108, A-8010 Graz, Austria

Received March 8, 2004. Revised Manuscript Received June 7, 2004

We investigate the oxidative degradation process occurring in ladder-type poly(*p*-phenylene) (LPPP) by spectroscopic and quantum-chemical techniques. Annealing experiments carried out for two representatives of the class of LPPP's with different side chains relate the change in emissive behavior of the polymer to the presence of ketonic defects on the main chain. The geometry, excitation, and emission energies as well as vibrational modes are calculated for model LPPP oligomers bearing these defects. The optical properties of these molecules are significantly changed compared to the pristine model systems. In the excited-state geometry, ketone-containing oligomers possess emissive excited states in the energy region of the experimentally observed low-energy emission band. The calculated infrared (IR) absorption peaks associated with the defects can also be correlated with the experimental IR spectra.

Introduction

Bridged poly(*p*-phenylene) polymers (PPP) have been extensively studied over the last 10 years. Good processability, high quantum efficiency of fluorescence, and blue emission make this class of materials promising candidates for high-efficiency polymer electroluminescent devices.[1]

However, one of the difficulties often encountered is that devices proved to be unstable during operation, gradually revealing a low-energy emission band in the range between 2 and 2.5 eV. This turns the desired blue color of EL into a greenish emission. The unwanted emission band was originally attributed to excimer or aggregate formation.[2,3] However, for poly(fluorene), which is one of the representatives of the class of bridged poly(*p*-phenylene)-type polymers, it has recently been shown that this change in emission color is rather related to oxidative degradation processes, giving rise to emissive on-chain defects.[4−10] In this work, we present results extending this finding to ladder-type poly(*p*-phenylene) (LPPP), as has already been suggested by Lupton.[11]

We studied two different types of ladder-type polymers by UV−vis and infrared spectroscopies in annealing experiments and complemented the experimental studies with quantum-chemical calculations. Our studies indicate that in LPPP various kinds of ketonic defects can be formed on the polymer chains during annealing. We discuss three different types of ketonic defects and calculate excitation and emission energies, oscillator strengths, and IR−absorption spectra of model oligomers bearing those defects.

The current work serves two purposes, namely, (i) to show that ketonic defects are responsible for the low-energy emission also in bridged ladder-type PPPs, implying that strained fluorene-type bridges are in general susceptible to oxidative degradation, and (ii) to provide evidence that (depending on the actual chemical

* To whom correspondence should be addressed. E.J.W.L. e-mail: e.list@tugraz.at. J.-L.B. e-mail: jean-luc.bredas@chemistry.gatech.edu. E.Z. e-mail: egbert.zojer@chemistry.gatech.edu.
† Georgia Institute of Technology.
‡ Institute of Nanostructured Materials and Photonics, Joanneum Research and Institute of Solid State Physics, Graz University of Technology.
|| Bergische Universität Wuppertal.
§ Institute of Solid State Physics, Graz University of Technology.

(1) Leising, G.; Grem, G.; Leditzky, G.; Scherf, U. *Proc. SPIE Int. Soc. Opt. Eng.* **1993**, *1910*, 70.
(2) Stampfl, J.; Tasch, S.; Leising, G.; Scherf, U. *Proc. Synth. Met.* **1995**, *71*, 2125.
(3) Lemmer, U.; Heun, S.; Mahrt, R. F.; Scherf, U.; Hopmeier, M.; Siegner, U.; Göbel, E. O.; Müllen, K.; Bässler, H. *Chem. Phys. Lett.* **1995**, *240*, 373.
(4) List, E. J. W.; Güntner, R.; Scandiucci de Freitas, P.; Scherf, U. *Adv. Mater.* **2002**, *14*, 374. Scherf, U.; List, E. J. W. *Adv. Mater.* **2002**, *14*, 477.
(5) Zojer, E.; Pongantsch, A.; Hennebicq, E.; Beljonne, D.; Brédas, J. L.; Scanducci de Freitas, P.; Scherf, U.; List, E. J. W. *J. Chem. Phys.* **2002**, *117*, 6794.
(6) Romaner, L.; Pogantsch, A.; Scandiucci de Freitas, P.; Scherf, U.; Gaal, M.; Zojer, E.; List, E. J. W. *Adv. Funct. Mater.* **2003**, *13*, 597.
(7) Lupton, J. M.; Craig, M. R.; Meijer, E. W. *Appl. Phys. Lett.* **2002**, *80*, 4489.
(8) Franco, I.; Tretiak, S. *Chem. Phys. Lett.* **2003**, *372*, 403.
(9) Gong, X.; Iyer, P. K.; Moses, D.; Bazan, G. C.; Heeger, A. J.; Xiao, S. S. *Adv. Funct. Mater.* **2003**, *13*, 325.
(10) Yang, X. H.; Neher, D.; Spitz, C.; Zojer, E.; Brédas, J. L.; Güntner, R.; Scherf, U. *J. Chem. Phys.* **2003**, *119*, 6832.
(11) Lupton, J. M. *Chem. Phys. Lett.* **2002**, *365*, 366.

10.1021/cm0496164 CCC: $27.50
Published on Web 07/27/2004

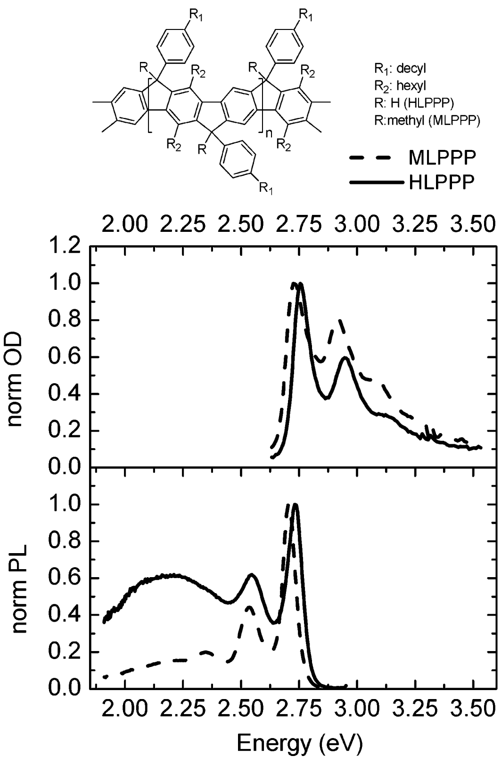

Figure 1. Photoluminescence (PL) (intensity per energy interval) and absorption (OD) spectra of HLPPP (solid line) and MLPPP (dashed line). The emission spectrum of HLPPP shows a low emission band in the energy range between 2.0 and 2.5 eV already prior to any heat treatment. The chemical structures of the two polymers are shown in the upper part of the figure.

nature of the investigated materials) there can be several types of emissive or nonemissive ketonic defects.

Methodology

Experimental. The two representatives of the ladder-type poly(*p*-phenylene)s used in this study were synthesized according to refs 12 and 13. Their chemical structures are shown in the upper part of Figure 1. Absorption spectra (optical density (OD)) were measured in a Perkin-Elmer λ9 transmission spectrometer. Photoluminescence (PL) spectra were taken with a Shimadzu RF5301PC spectrofluorometer, whose spectral response has been calibrated using a tungsten−halogen light source (Ocean Optics LS-1-CAL). Infrared (IR) spectra were recorded by a BOMEM FTIR (MB-102) spectrometer. In all emission spectra shown below, the normalized (norm.) intensity per energy interval is plotted.

We investigated the growth of the low emission band in photoluminescence by annealing polymer films at 120 °C under vacuum (10^{-5} mbar) and in air while covering the samples with aluminum foil to avoid light exposure. The heating was performed on hotplates. After defined time intervals (see legend of Figure 4), photoluminescence and infrared absorption were measured. For the PL measurements, the films were spin cast onto a quartz substrate. Their optical densities at the absorption maximum were between 0.1 and 0.2 in order to reduce reabsorption. The samples suitable for IR spectra (optical densities higher than 4) were drop cast onto CaFl substrates.

Calculations. Vibrational Modes. The ground-state total energies, equilibrium geometries, eigenfrequencies, and normal coordinates were calculated at the density functional theory (DFT) level using the Gaussian-98 program package.[14] For the exchange functional, we used the modified Perdew−Wang (mPW) expression developed by Adamo et al.;[15] the correlation functional was Lee, Yang, and Parr's (LYP).[16] We chose the split-valence 4-31G**[17,18] basis-set, which includes two sets of higher angular momentum polarizing functions. This level of theory was found to provide a very reliable description of the vibrational properties of oligo(phenylene)s.[19]

Optical Properties. The methodology for describing the absorption and emission of conjugated polymers has been successfully applied in numerous previous studies (see, e.g., refs 5, 20, and 21). Transition energies and oscillator strengths were calculated on the basis of the semiempirical Hartree−Fock intermediate neglect of differential overlap (INDO) method[22] using Gaussian-98.[14] Electron correlation effects in the excited states were included via a single configuration interaction (SCI) technique, scaling the CI active space with the number of carbon atoms in the π-conjugated backbone. To better understand the nature of the excited states, we used the results of the INDO/SCI calculations to calculate two-dimensional electron−hole pair distributions. Here (in contrast to previous studies),[5,21] we adopt a non-anti-symmetrized definition of the electron−hole pair distributions, in analogy to refs 23−25. It can be shown that this provides a more appropriate representation of the properties of the electron−hole pairs.[26]

The geometries of the molecules in their electronic ground state are optimized with the semiempirical Hartree−Fock Austin model 1 (AM1) method, as the model systems for studying optical properties were much larger than those for the vibrational simulations (vide infra).[27] To consider geometry-relaxation effects in the excited state, the AM1 Hamiltonian is coupled to a configuration interaction (CI) approach, as implemented in the AMPAC program package.[28] The CI space was chosen according to the dominant terms of the SCI expansion of the lowest excited states in the ground-state geometry; oligomer L10, HOMO-3 to LUMO+3; oligomer C10, HOMO-17 to LUMO+3; oligomer Po10, HOMO-19 to LUMO+10; oligomer Pa10, HOMO-1 to LUMO+10; oligomers are denoted as shown in Figure 4 (note that the input geometry for an excited-state geometry calculation is the output geometry of the corresponding ground-state AM1 calculation).

Results and Discussion

Experimental Investigations. We present experimental results obtained for two representatives of the class of ladder-type poly(*p*-phenylene)s, MLPPP and HLPPP. The difference between the two molecules

(12) Scherf, U.; Müllen, K. *Makromol. Chem., Rapid Commun.* **1991**, *12*, 489.
(13) Scherf, U.; Bohnen, A.; Müllen, K. *Makromol. Chem., Rapid Commun.* **1992**, *193*, 1127.
(14) Frisch, M. J.; Trucks, G. W.; Schlegel H. B. et al. *Gaussian 98*, Revision A.9; Gaussian, Inc.: Pittsburgh, PA, 1998.
(15) Adamo, C.; Barone, V. *J. Chem. Phys.* **1998**, *108*, 664.
(16) Lee, C.; Yang, W.; Parr, R. G. *Phys. Rev. B* **1988**, *37*, 785.
(17) Ditchfield, R.; Hehre, W. J.; Pople, J. A. *J. Chem. Phys.* **1971**, *54*, 724.
(18) Pietro, W. J.; Francl, M. M.; Hehre, W. J.; DeFrees, D. J.; Pople, J. A.; Binkley, J. S. *J. Am. Chem. Soc.* **1982**, *104*, 5039.
(19) Heimel, G.; Somitsch, D.; Knoll, P.; Zojer, E. *J. Chem. Phys.* **2002**, *116*, 10921.
(20) Cornil, J.; Beljonne, D.; Brédas, J. L. *J. Chem. Phys.* **1995**, *103*, 834. Cornil, J.; Beljonne, D.; Brédas, J. L. *J. Chem. Phys.* **1995**, *103*, 842.
(21) Zojer, E.; Buchacher, P.; Wudl, F.; Cornil, J.; Calbert, J. Ph.; Brédas, J. L.; Leising, G. *J. Chem. Phys.* **2000**, *113*, 10002.
(22) Pople, J. A.; Beveridge, D. L.; Dobosh, P. A. *J. Chem. Phys.* **1967**, *47*, 2026. Zerner, M. C.; Loew, G. H.; Kichner, R.F.; Mueller-Westerhoff, U. T. *J. Am. Chem. Soc.* **1980**, *102*, 589.
(23) Mukamel, S.; Tretiak, S.; Wagersreiter, T.; Chernyak, V. *Science* **1997**, *277*, 781.
(24) Tretiak, S.; Mukamel, S.; *Chem. Rev.* **2002**, *102*, 3171.
(25) Rissler, J.; Bässler, J. H.; Gebhard, F.; Schwerdtfeger, P. *Phys. Rev. B* **2001**, *64*, 45122.
(26) Romaner, L. et al. Manuscript in preparation.
(27) Dewar, M. J. S.; Zoebisch, E. G.; Healy, E. F.; Stewart, J. J. P. *J. Am. Chem. Soc.* **1985**, *107*, 3902.
(28) *AMPAC 5.0 User's Manual*; Semichem: Shawnee, KS, 1994.

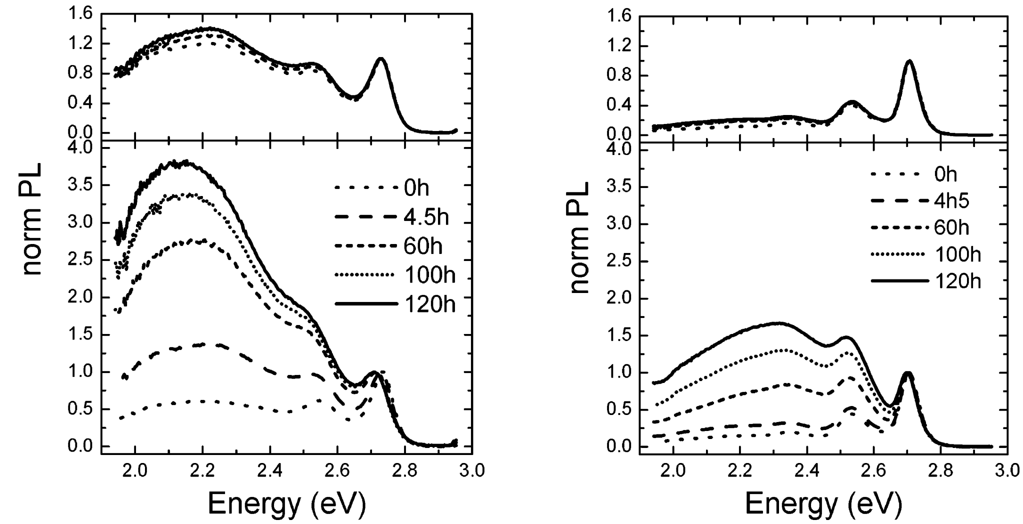

Figure 2. Evolution of photoluminescence spectra (intensity per energy interval) of HLPPP (left) and MLPPP (right) for annealing in vacuum (upper graph) and ambient atmosphere (lower graph). Samples were kept at 120 °C for the times specified in the legend, and light exposure was avoided. The spectra are normalized to the peak at 2.7 eV.

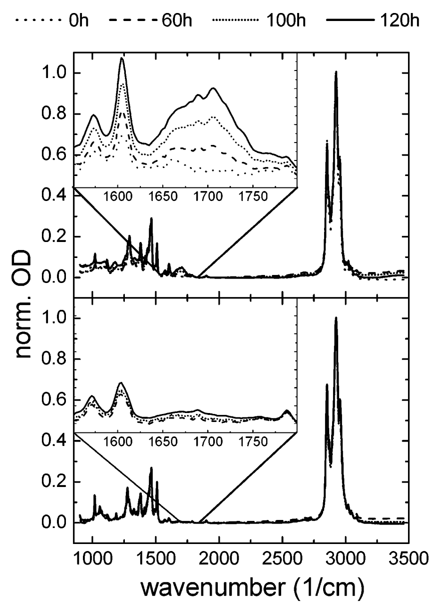

Figure 3. Evolution of IR spectra of HLPPP (upper graph) and MLPPP (lower graph) for annealing in ambient atmosphere. Samples were kept at 120 °C for the times specified in the legend, and light exposure was avoided.

resides in one of the side chains at the bridge; HLPPP has a hydrogen atom, while in MLPPP the hydrogen is replaced by a methyl group (see top of Figure 1).

The luminescence and absorption spectra of HLPPP and MLPPP prior to heat treatment are displayed in Figure 1. In absorption, the vibronic structure of the two materials is very similar; a slight red shift can be observed for MLPPP. We attribute this to a higher effective conjugation length in this material. The vibronic progression observed for the materials both in emission and absorption is due to coupling between the electronic excitation and C−C stretching vibrations of the backbone. In addition to the emission between 2.5 and 2.8 eV, HLPPP displays a broad emission band between 2.0 and 2.5 eV.

The properties of this low emission band are further investigated in annealing experiments. The results are shown in Figure 2. In photoluminescence, HLPPP displays a strong increase of the low emission band when the samples are heated in air. When the heating is performed in a vacuum (10^{-5} mbar), only very small changes of the emission spectra are observed. This implies that, in analogy to the observations made for polyfluorenes,[4] the incorporation of oxygen in the macromolecule rather than ordering effects during annealing is responsible for the appearance of the low-energy emission. Qualitatively, MLPPP shows a similar behavior but the degree of degradation for equivalent annealing times is significantly reduced. This result also points toward a chemical degradation rather than a morphological modification of the polymer films since the methyl group at the bridge is chemically more stable than the hydrogen.

Assignment of the emissive species to intrachain ketonic defects is further supported by the infrared spectra shown in Figure 3, which were recorded on samples subjected to the same heat treatment as the samples for the PL spectra. The increase in intensity of the C=O stretching mode (located in the 1630−1750 cm^{-1} region) during annealing is clearly observed. Again, it is much more pronounced for HLPPP (top graph) than for MLPPP (bottom graph). Since MLPPP and HLPPP differ in their chemical structure only at the bridge, these results suggest that the C=O signature is related to ketonic defects located at the bridge rather than on the side chains. Since the IR−absorption spectra of HLPPP display several well-separated peaks and shoulders between 1630 and 1750 cm^{-1}, it appears that, upon degradation, several distinct and well-defined types of ketonic defects are formed.

Here, two different defect-forming mechanisms are proposed for the degradation mode of the polymer film, Scheme 1. During the operation of a polymer light-emitting diode (PLED), charging of the chain can cause loss of the hydrogen atom at the bridge where an oxygen molecule can attack. On the other hand, when the sample is subjected to heat treatment or ultraviolet (UV) irradiation, it is possible that the oxygen molecule directly attaches to the bridge to form a carboxylic group. At that point, the carbon atom at the bridge is surrounded by three phenylene units and the bond from

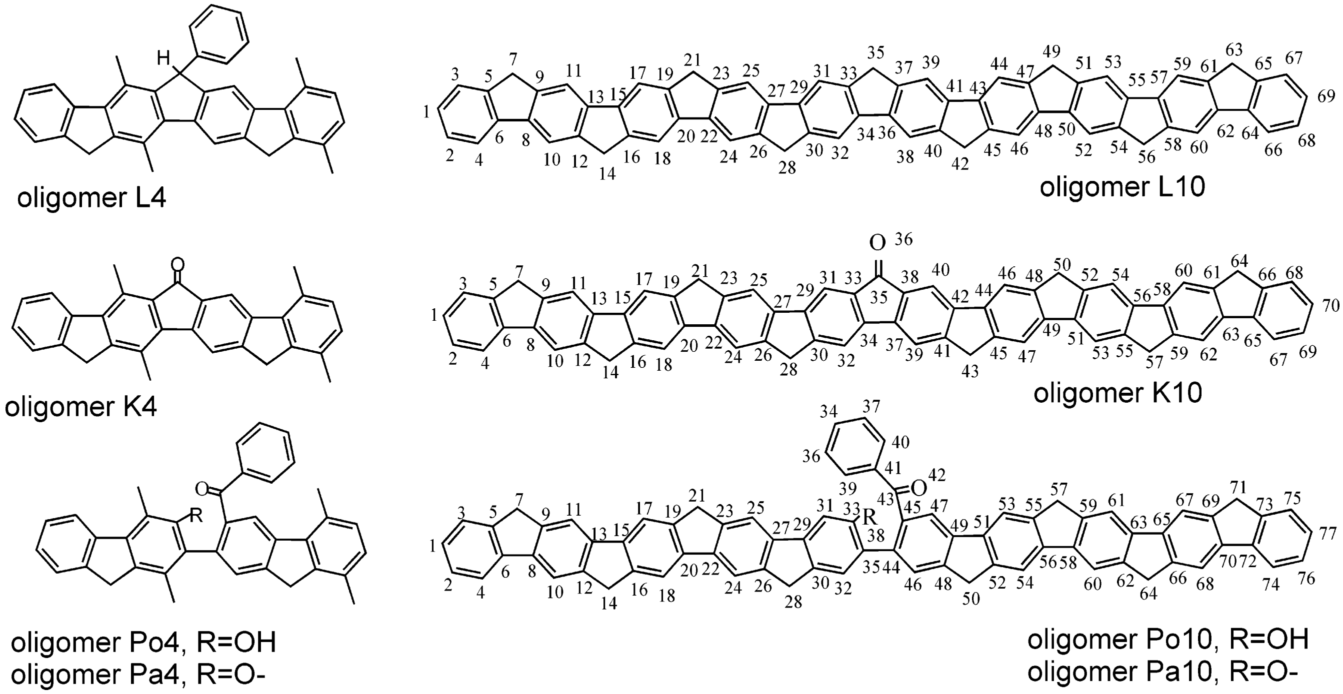

Figure 4. Model oligomers considered in the calculations. Four-ring systems are chosen for the calculation of the vibrational modes and 10-ring systems for the calculations of the optical properties.

Scheme 1. Defect Formations in the Ladder-type Polymer

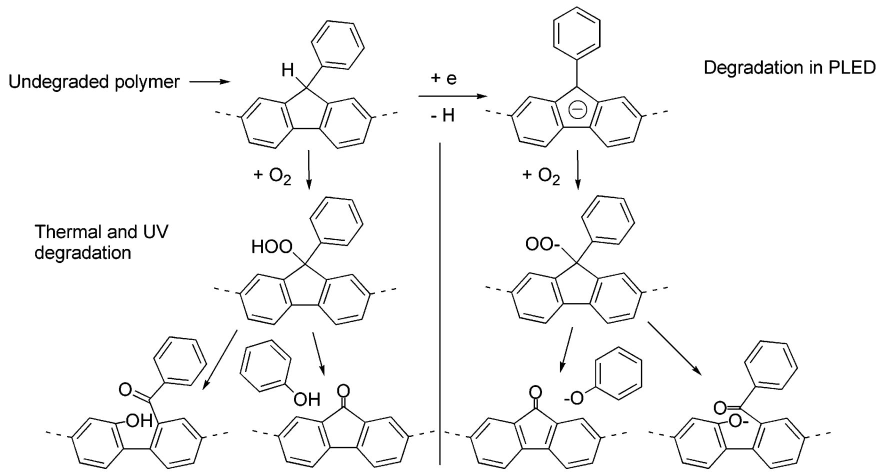

the bridge carbon to any of the surrounding rings can break during oxidation. Thus, three chemically distinct defects can be formed in LPPP (with the possibility of combinations of those defects on neighboring bridges): The first type, referred to as the ketonic defect, is generated when the aromatic ring of the side chain is clipped off the backbone and the oxygen remains attached to the bridge via a double bond; this defect corresponds to the defect proposed in ref 4 for polyfluorene. Other types of defects, referred to as the phenol defect and the phenolate defect, are formed when one of the bonds to the backbone rings breaks. In this case, chemical intuition suggests that two oxygen atoms remain attached to the backbone; one is doubly bonded to the original bridge carbon atom, while the other is attached directly to one of the backbone phenylene rings to form a $-OH$ or $-O^-$ group. In the former case, the molecule remains neutral, while in the latter the molecule is negatively charged. The ketonic and the phenol defects are expected to be formed when degrading by annealing or UV irradiation, while PLED operation should lead to ketonic defect and phenolate defects. (We emphasize that even though all types of defects bear a ketonic group, we refer to only one of the defects as the “ketonic defect”,)

Quantum-Chemical Calculations. To gain a better understanding of the experimental data, we performed quantum-chemical calculations on the model oligomers shown in Figure 4, which bear the three types of defects. For the simulation of the IR spectra, we considered systems with four rings in the backbone; for the emission and absorption properties, we investigated 10-ring systems to remain consistent with our earlier work.[5] While the side chains (R_1 and R_2 in the inset of Figure 1) have hardly any effect on the optical spectra, their influence on the details of vibrational properties is more significant. Therefore, we have substituted the side chains by H atoms in the calculations of the optical properties while we model them as methyl groups in the vibrational studies. All oligomers, including those bearing the phenolate defect, are closed-shell systems.

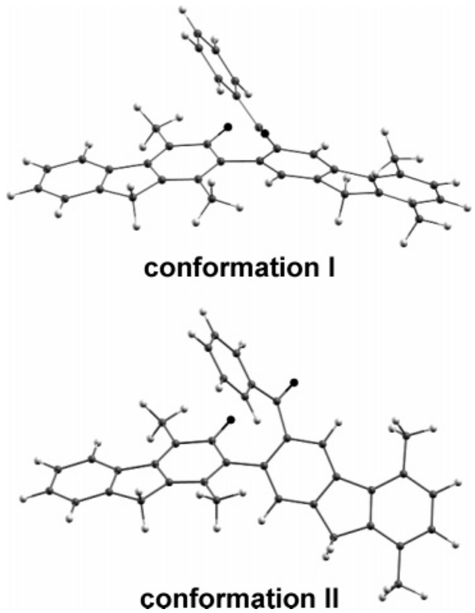

Figure 5. Oligomer Pa4 in two possible ground-state geometries (the oxygen atoms are colored black, the carbon gray, and the hydrogen atoms white). For both oligomers the C═O group is (nearly) in plane with the phenyl ring of the side chain.

Geometric Structures. Geometry optimizations indicate that molecules bearing the ketonic defect remain flat since the degradation just substitutes the two side chains by a doubly bonded oxygen. The phenol and phenolate defects, however, cause the backbone to twist at the defect point, since the two adjacent rings are no longer planarized by a bridge and the steric hindrance between the remaining groups at the broken bridge is large. For molecules Po4, Pa4, Po10, and Pa10 bearing these defects, we find two possible geometrical conformations in which the total energy is in a local minimum. They are illustrated in Figure 5 for Pa4. In conformation II, the oxygen atoms point in the same direction, while in conformation I, the ketonic oxygen is rotated together with the sidechain by approximately 180°. For the other molecules, the situation is qualitatively the same.

IR−Absorption. The calculated IR spectra of the model molecules are shown in Figure 6. The approximations we made (shortened backbone and reduced length of side chains) are expected to result in slightly different theoretical results vs experiment, since backbone modes are delocalized over the whole chain. The C═O stretching mode on the other hand is localized around the oxygen atom (see displacement in the inset of Figure 6) and is, therefore, not significantly affected by our choice of model systems.

The C═O stretching mode is calculated at 1699 cm^{-1} for oligomer K4, at 1660 cm^{-1} for oligomer Po4 (conformation I), and at 1625 cm^{-1} for oligomer Pa4 (conformation I). The stretching modes for the latter two oligomers in conformation II are centered at 1626 and 1627 cm^{-1}, respectively. In the actual films, it can be expected that part of the molecule bearing the phenol or phenolate defects adopts a large number of possible orientations, that all display the C═O stretching mode at slightly different wavenumbers. This is consistent with the extension of the experimentally observed C═O signature over a range of 120 cm^{-1}.

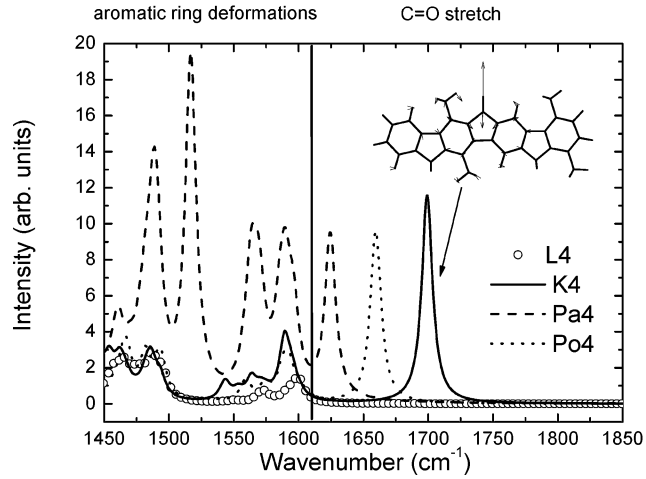

Figure 6. Calculated infrared spectra for the model molecules. The calculated vibrational features are broadened by a Lorentzian function with a full-width at half-maximum of 10 cm^{-1}. The inset shows the displacement pattern of the C═O stretching mode of molecule K4. Peaks related to aromatic ring deformations are found below 1610 cm^{-1}; peaks related to the C═O group are located above 1610 cm^{-1}. The spectra of Pa4 and Po4 are shown for conformation I.

The results of the calculations allow the identification of the peaks between 1550 and 1600 cm^{-1} as deformations of the aromatic rings of the backbone. The calculated oscillator strengths of these modes increase for all degraded molecules, which is in agreement with experiment (see the inset in the upper graph of Figure 3).

Phenolate defects show, due to the charging of the molecule, additional features in the calculated spectra in the energy range between 1450 and 1550 cm^{-1}. We found no evidence for such features in the experimental spectra, which indicates that indeed the phenolate defect is not formed in the film upon annealing.

Optical Properties. Electronic transition energies (corresponding to vertical transitions) and oscillator strengths for the lowest-lying excited states of oligomers L10, K10, Po10 (conformation I), and Pa10 (conformation I) are depicted in Figure 7. These values were calculated for both the ground-state geometry (GSG) and the geometry of the lowest excited state (ESG) to simulate both absorption and emission. To further analyze the nature of the relevant excited states and to describe their extension in real space, the electron−hole pair distribution is shown in Figure 8. The plots are similar for the same states in the GSG and ESG, the difference being a confinement of the excitation due to vibrational relaxation.[29] This effect is rather small and not relevant to the main focus of our investigations.

Pristine Molecule. The pristine polymer is represented by oligomer L10. There the lowest-lying singlet excited state is a strongly optically allowed $\pi-\pi^*$ state. As a result of the geometry relaxation in the excited state, the vertical transition for emission is shifted by 0.29 eV to lower energies. The electron−hole plot of the lowest excited state in Figure 8 shows a regular pattern reflecting the periodicity of the backbone. The excited

(29) Tretiak, S.; Saxena, A.; Martin, R. L.; Bishop, A. R. *Phys. Rev. Lett.* **2002**, *89*, 97402.

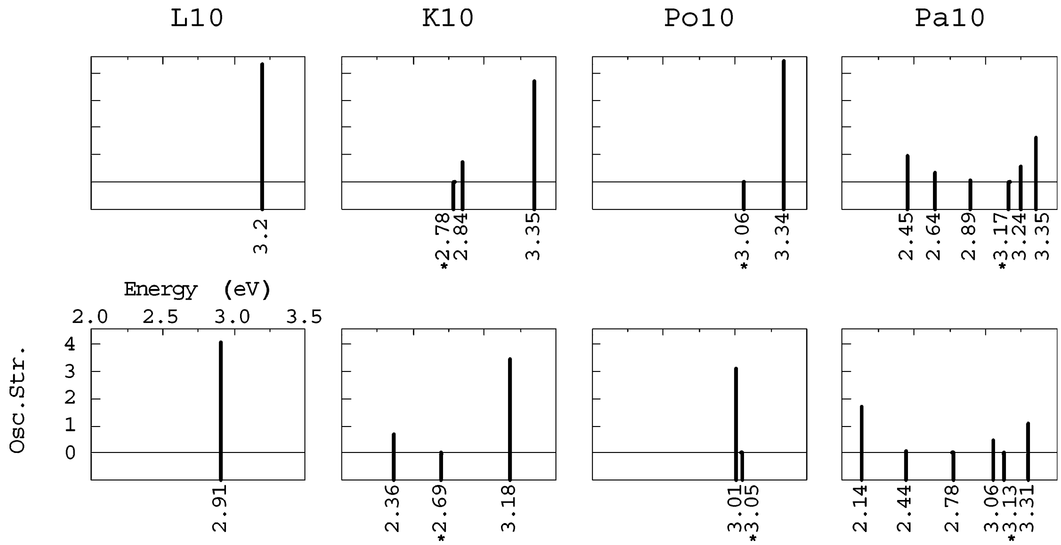

Figure 7. Energetic positions and oscillator strengths of the excited states of the model oligomers in their ground-state geometry (upper graphs) and relaxed excited-state geometries (lower graphs). "Osc. Str." denotes oscillator strength. For the sake of clarity, scale and axis labels are given only for the graph in the bottom left corner. Scales and axis labels for the other graphs are identical. In the relaxed excited-state geometry, the states shift toward lower energies while the relative ordering of the excited states stays the same. The exception are the n$-\pi^*$ states, which stay at almost the same energy and, consequently, exchange position with states lying slightly higher in energy in the GSG. Therefore, the n$-\pi^*$ states are denoted by an asterisk.

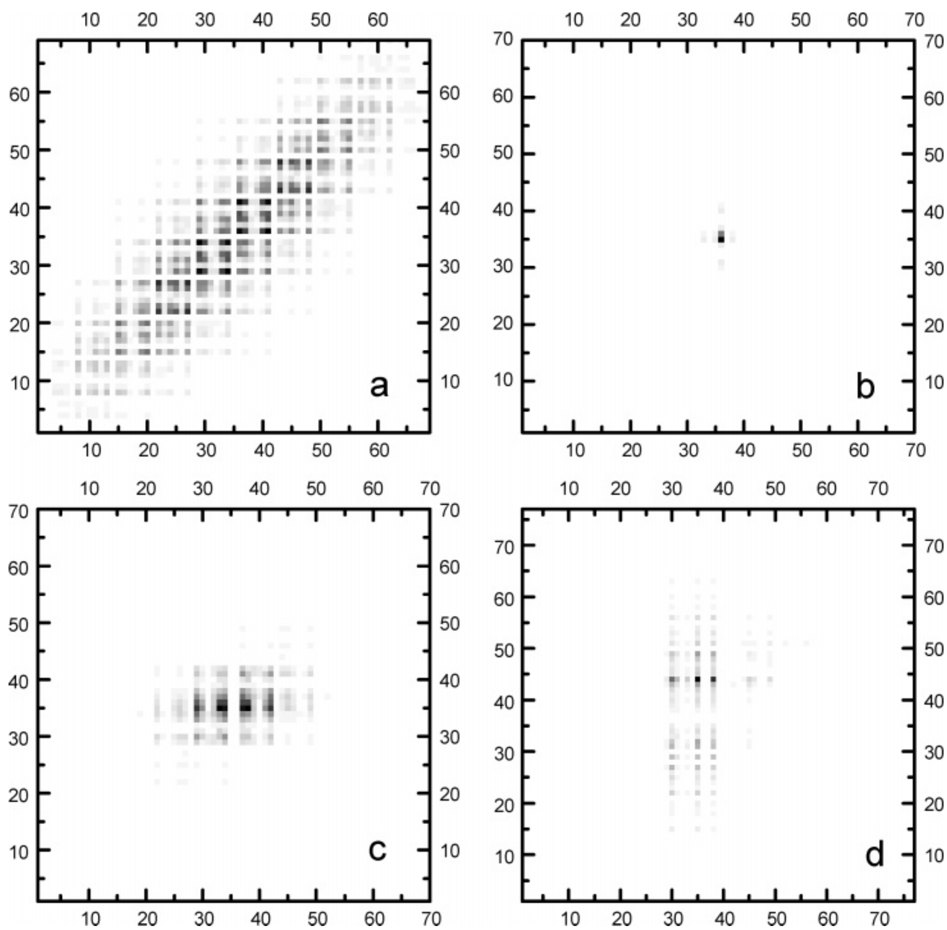

Figure 8. Probability of finding the electron and simultaneously the hole at two specific sites of the molecule. The x-axis refers to the position of the hole and the y axis to the position of the electron. Every number on the axes corresponds to an atom on the molecules as specified in Figure 4. All molecules are in their ground-state geometry. (a) First excited state of molecule L10. (b) n$-\pi^*$ state of molecule K10. (c) CT $\pi-\pi^*$ state of molecule K10. (d) First excited state of molecule Pa10 in conformation I.

state is delocalized over the whole backbone and therefore significantly influenced by chain length.[30]

Ketonic Defect. The $\pi-\pi^*$ state of the pristine oligomer is found (in a slightly modified form) in the degraded molecule K10 as the third excited state. Energetic position, oscillator strength (Figure 7), and

(30) Zojer, E.; Cornil, J.; Leising, G.; Brédas J. L. *Opt. Mater*. **1999**, *12*, 307.

extension in the electron−hole plot (not shown) are similar to the first excited state of L10. The presence of the doubly bound oxygen, however, introduces two new excited states that lie lower in energy than the $\pi-\pi^*$ state. The nature of these states has been already discussed in detail in the case of polyfluorene in refs 5 and 8. They were identified as a n−π^* state and a charge transfer (CT) $\pi-\pi^*$ state. The former is optically forbidden from the ground state and, as Figure 8b shows, is strongly localized on the ketonic defect. Its energetic position is, therefore, almost unaffected by the geometry relaxation. The CT $\pi-\pi^*$ state is optically allowed with a moderate oscillator strength and becomes the lowest excited state after geometry relaxation. As shown in Figure 8c, it is localized as well around the defect site of the molecule.

Phenol Defect. In this case, only two states appear below 3.35 eV in both conformations: a delocalized $\pi-\pi^*$ state and the n−π^* state. Figure 7 shows that these two states lie very close in energy (around 3.0 eV) after geometry relaxation. The electron−hole plot of the n−π^* state is nearly identical to the electron hole plot of the n−π^* state in K10 (Figure 8b). Its energetic position is, however, blue shifted by ca. 0.3 eV, and its oscillator strength is not strictly zero, which is attributed to the fact that the O10 molecule is not flat and thus presents a lower symmetry. Also, the $\pi-\pi^*$ state is blue-shifted compared to molecule L10 since conjugation is reduced at the defect point.

Since both states lie higher in energy than the lowest excited state of the pristine polymer, energy-transfer processes in the film deplete them. These defects are, therefore, not relevant for the emissive properties. The same holds true for the oligomers in conformation II, where the $\pi-\pi^*$ and n−π^* transitions are both situated at 3.04 eV in the relaxed geometry as well as for the defect located at the end of the model system.

Phenolate Defect. The order of the excited states is somewhat modified in molecule Pa10. Figure 7 shows six excited states in the energy range between 2.00 and 3.5 eV. The fourth excited state in the GSG, which becomes the fifth excited state in the ESG, can again be identified as an n−π^* state with the same characteristics as the n−π^* state in oligomer Po10. The electron−hole plot for the lowest excited state is shown in Figure 8d. Its shape implies a hole localization on the phenyl ring the O− is attached to. The electron is delocalized over several rings. The pronounced maximum in this electron−hole plot is for the hole on site 35 and the electron on site 44. Thus, the exciton is found mostly in the center of the oligomer backbone. The state is optically allowed and lower in energy than the lowest exited state of the ketonic defect.[31] Calculations for the oligomer in conformation II and for the defect at the end of the molecule in conformation I give lowest excited-state energies of 2.11 (1.65 oscillator strength) and 2.29 eV (1.01 oscillator strength).

In the following, we discuss the implications of the results of the calculations on the model oligomers for the optical properties for the degraded ladder-type polymer film. It has to be stressed that the calculations do not aim at representing the exact emission and absorption energies but rather at investigating the new features introduced by the defects.

Defect concentration is typically very low in the polymer;[6] therefore, the pristine conjugated segments dominate the absorption in the polymer. Comparison of the results obtained for molecule L10 with the experimental values in Figure 1 shows that absorption and emission energies are higher in the calculations, which is expected[30] since the oligomer is shorter than the conjugated segments in the actual polymers. The band gap of the pristine system can be determined from Figure 1 and is located around 2.75 eV.

As a result of excitation energy migration, the luminescence of a polymer is highly sensitive to even very small concentrations of defects when they form intragap states. This is indeed the case for the ketonic and phenolate defects. Therefore, we propose that these two types of defects can be held responsible for the low emission band observed between 2.0 and 2.4 eV upon device degradation and thermal annealing. On the other hand, the presence of the phenol defect has no influence on the optical properties of the film.

Conclusions

We studied two representatives of ladder-type poly(*p*-phenylene)s, HLPPP and MLPPP, by annealing experiments. Samples were heated in a vacuum and under ambient atmosphere while avoiding light exposure. The increase of the contribution of the low emission band around 2.2 eV relative to the emission of pristine LPPP at 2.75 eV can be related to an increase in concentration of ketonic defects, which was monitored by infrared spectroscopy. We found that HLPPP degrades much more rapidly than MLPPP, which can be attributed to reduced chemical stability.

To help in the interpretation of the PL and IR spectra, quantum-chemical calculations were carried out on model oligomers. The fine structure of the IR spectra in the region of the C=O stretching vibration indicates that there are several types of well-defined ketonic defects present in degraded LPPP. Therefore, we studied three different types of oxidative defects which can be formed in the polymer upon annealing or during device operation. We refer to them as ketonic, phenolate, and phenol defects. The ketonic defect does not affect the integrity of the bridge, while the phenolate and phenol defects break one of the bonds of the bridge. All types of defects are associated with C=O stretching vibrations between 1625 and 1699 cm^{-1}, and the ketonic and phenolate defects have low-lying excited states that emit in the green-orange spectral region with a moderate oscillator strength.

Our findings support the view that the bridge can be subject to oxidative degradation in all polymers containing fluorene units, with the possible consequence of low-energy emission bands. Therefore, synthetic strategies need to address the problem of chemical stability, e.g., by ensuring that no monoalkylated substituents are present at the bridge.[32]

(31) We can, therefore, expect to observe the low emission band in EL at lower energies than in PL. Preliminary experimental results carried out for HLPPP indeed show a slight red shift of the low emission band.

(32) Craig, M. R.; De Kok, M. M.; Hofstraat, J. W.; Schenning, A. P. H. J.; Meijer, E. W. *J. Mater. Chem.* **2003**, *13*, 2861.

Acknowledgment. The authors wish to thank Stephen Barlow for valuable suggestions regarding defect formation. The work at Georgia Tech is partly supported by the U.S. National Science Foundation (through the STC for Materials and Devices for Information Technology Research and through CHE-0342321) and the Georgia Tech Center for Organic Photonics and Electronics. H.W. acknowledges the financial support by the Spezialforschungsbereich Elektroaktive Stoffe (Project F917) and G.H. by project No. P14237-PHY of the Austrian Fonds zur Förderung der Wissenschaftlichen Forschung. Christian Doppler Laboratory—Advanced Functional Materials is a key member of the long-term research strategies of AT&S.

CM0496164